This article has been accepted for publication in a future issue of this journal, but has not been fully edited. Content may change prior to final publication. Citation information: DOI 10.1109/TPEL.2016.2581828, IEEE Transactions on Power Electronics



# Precise Color Control of Red-Green-Blue Light-Emitting Diode Systems

Huan-Ting Chen, Siew-Chong Tan, *Senior Member*, Albert. T. L. Lee, *Member, IEEE*, De-Yan Lin , *Member, IEEE, IEEE,* S. Y. (Ron) Hui, *Fellow, IEEE*

***Abstract*—The complex nature and differences of the luminous and thermal characteristics of red, green and blue (RGB) light-emitting diodes (LEDs) make precise color control of RGB LED systems a great technological challenge. This paper presents a nonlinear model that includes coupling effects among LED devices for predicting color in RGB LED systems. A control method is included to demonstrate that this model can be used for precise color control. The proposed model and control method have been successfully evaluated in practical tests. The measurements agree well with model predictions. They form a new design tool for precise color control of RGB LED systems.**

***Index Terms*—Lighting system, photo-electro-thermal (PET), Red-Green-Blue (RGB) light-emitting diodes (LED) system, Color control.**

## I. INTRODUCTION

Unlike traditional light sources such as incandescent lamps and discharge lamps, light-emitting diode (LED) has the properties of wide color gamut and high color saturation. For white light generation, one method is to use light from a blue LED to excite yellow phosphor to obtain white light. Another method is to use red, green, and blue (RGB) LEDs for coloring mixing. RGB LED systems can vary color in wide chromatic range and has been applied in architectural, commercial and residential lighting. Companies such as Philips Lighting and Osram Opto-semiconductors developed color-tunable Hue bulbs, although the preciseness of color control is still far from satisfactory.

As red, green and blue LEDs have different thermal and luminous characteristics, variation in one color can have a siginificant effect on the targeted color point. Color control in RGB LED systems is a multidisciplinary subject involving electric power, circuit topology, thermal management, and optical performance [1], [2]. The RGB LED systems also face thermal challenges because of their usual requirements for high compactness [3],[4].

Manuscript received May 22, 2016. This work is supported by the Hong Kong Research Grant Council under Theme-based Research Project: T22-715-12N

H. T. Chen, S. C. Tan, Albert. T. L. Lee and D. Y. Lin are with the Department of Electrical & Electronic Engineering, The University of Hong Kong (email: htchen23@ gmail.com, sctan@eee.hku.hk, tlalee@eee.hku.hk, deyanlin@eee.hku.hk).

S.Y. R. Hui is with the Departments of Electrical & Electronic Engineering, The University of Hong Kong (email: ronhui@eee.hku.hk) and Imperial College London (e-mail: r.hui@imperial.ac.uk).

A typical RGB LED system usually requires each type of LED to be driven by either a dedicated LED driver or one channel of a multichannel LED driver. RGB LED color tuning can be achieved by PWM modulation of the current in each type of LED [5]. Linear power supplies or switched-mode power supplies can be used to drive the LEDs. The energy efficiency of linear power supply system is low. Although the efficiency of switched-mode power supply system is high, three independent power supplies are required to drive the RGB LEDs with proper current control schemes. This is redundancy in three independent converter control circuits in the power supplies [6]. To resolve the redundacy issue, a single-inductor multiple-outputs converter topology has been rcently proposed for driving single or multiple color LED strings in order to reduce the form factor and increase the power density [7][8]. The performance of RGB LED systems, such as illumination intensity and color, is determined by the luminous ratio of RGB colors. For high-end applications, it is necessary to maintain the LED color point even when LED junction temperature changes with dimming level and ambient temperature. Color control methods for RGB LED systems based on voltage-junction temperature curve and current-voltage empirical model have previously been reported [9] [10]. In [11], a lookup table was used as the multivariable robust control to compensate for the variation of junction tempreature to regulate the color and luminous intensity outputs of RGB LED lighting system. However, the illuminations of LEDs change with junction temperature due to self-heating of LEDs and variation of ambient temperature. Hence, the thermal coupling effect will affect both luminous intensity and color of LED [12]. Precise color control of RGB LED systems remains a grand challenge in lighting technology.

Recently, a non-linear empirical model of the bi-color white LED system for high-quality dimming and correlated color temperature (CCT) control of the system has been proposed [13]. It was demonstrated that precise control of color mixing between warm-white and cool-white LEDs is possible [14]. Building upon the basic concept in [13], this paper presents a coupled tri-color model and proposes a precise color control method for RGB LED systems. Color deviation of a tri-color LED system arising from current and temperature changes is more complicated than that of a bi-color LED system. The control variables of the bi-color LED system are correlated color temperature (CCT) and luminous flux of two individual LED sources, and the total variables are four. For the RGB LED systems, the control parameters are tri-stimulus values of blue, green and red LED sources, and so there are a total of nine variables. Despite the complexity of the tri-color model (reflecting the complex nature of light science), the proposed

This article has been accepted for publication in a future issue of this journal, but has not been fully edited. Content may change prior to final publication. Citation information: DOI 10.1109/TPEL.2016.2581828, IEEE Transactions on Power Electronics



control method can be easily implemented in digital controller. The model predictions and measured results are included to demonstrate the validity of the tri-color model and control method.

## II. The COLOR STAILITY OF RGB LED SYSTEMS

The CIE 1931 color system is the root of colorimetry. The tristimulus values X, Y and Z can be normalized as:

$$\begin{cases} x = \dfrac{X}{X+Y+Z} \\ y = \dfrac{Y}{X+Y+Z} \\ z = \dfrac{Z}{X+Y+Z} \end{cases} \quad (1)$$

The CIE 1931 chromaticity diagram (Fig. 1) does not represent color gradations in a uniform matter. Therefore, CIE 1931 color space could be transformed into CIE 1960 Uniform Chromaticity Space (UCS), which has more uniform $u$ and $v$ coordinates. The variables $u$ and $v$ can be derived from the tristimulus values $X$, $Y$ and $Z$ as follows:

$$\begin{cases} u = \dfrac{4X}{X+15Y+3Z} \\ v = \dfrac{6Y}{X+15Y+3Z} \end{cases} \quad (2)$$

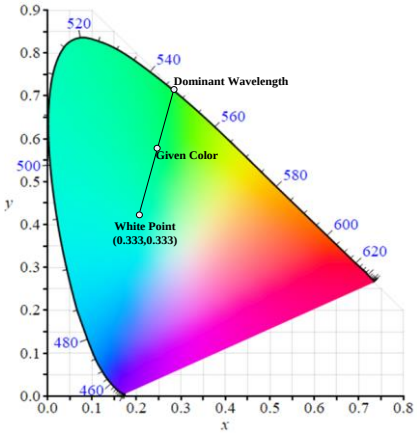


Fig 1 The CIE 1931 color space chromaticity diagram

Conventional light sources can be manufactured with their consistent light ouput and color. CIE 1960 UCS color system ($u$,$v$) is commonly used to analyze color deviation. To quantify the color deviation of a light source, the value $\Delta uv$ is defined as

$$\Delta uv = \sqrt{(u-u_0)^2 - (v-v_0)^2} \quad (3)$$

where ($u$,$v$) is the color coordinates of the light source, and ($u_0$,$v_0$) is the required color coordinates. This is the distance in ($u$,$v$) color space of the light source from the targeted color point. Fluorescent lamps are usually specified to be within $\Delta uv$=0.003 of the targeted color point [15]. The color tolerance specifications for LED sources are listed in [16].

### *A Issues about color stability*

A major influence on color properties of a RGB LED system is the variation on the light output of individual LED sources. This can be attributed to the coupled thermal effects on the LED sources. An experimental setup (Fig. 2) has been used to illustrate this point. The LED sources under test are mounted to a Peltier-cooled fixture (with 10 W heat-sinking capability and being used as a temperature-controlled heatsink), which is attached to an integrating sphere in accordance with the recommendations of CIE. The Peltier-cooled fixture is used to stabilize the LED temperature for the optical measurements and also serves as an actively temperature-controlled cold-plate for thermal measurements. The LED sources are fixed on temperature-controlled heatsink by thermal adhesive with high thermal conductivity. The optical measurements of the LED sources are performed under the steady-state thermal and electrical conditions using the TeraLED & T3Ster system. Apart from the thermal and optical measurements, all temperature-dependent parameters of the LED (such as optical power, luminous flux, chromaticity coordinates, etc.) are measured and recorded. The light output and transient thermal curves are measured only after 20 minutes of driving the LEDs while the heatsink temperature is kept constant.

Tests have been conducted to evaluate the effects of changing the power of one type of LED on the RGB LED system. The variations of the measured chromaticity coordinate ($x$,$y$) of the RGB LED system are shown in Fig. 3, while the variations of the dominant wavelength of the LED lamp are included in Fig. 4. The test procedures are:

1. The red, blue and green LEDs are housed inside a lamp fixture.
2. Inject the same current of 0.35 A into red, blue and green LEDs.
3. Decrease the current of blue LED from 0.35 A, while keeping the currents of the red and green LEDs at 0.35 A.
4. The variations of the total optical power, chromaticity coordinates (x,y), dominant wavelength of LED lamp (integrated the blue, red and greed LED sources) are measured and displayed as the respective “blue curves” in Figs 3 and 4.
5. Repeat Step 1 and Step 2. Vary the current of the green LED from 0.35 A, while keeping the currents of red and blue LEDs at 0.35 A. Then plot the respective results in Figs. 3 and 4 as the respective “green curves”.
6. Repeat Step 1 and Step 2. Vary the current of the red LED from 0.35 A, while keeping the currents of green and blue LEDs at 0.35 A. Then plot the respective results in Figs. 3 and 4 as the respective “red curves”.

Fig. 3 shows that, at a required color point ($x$,$y$) of (0.3474,0.2345), the variation range of the chromaticity coordinates ($x$,$y$) of a RGB LED system is very large with a change of less than 10% in light intensity of red, green or blue LEDs. Fig. 4 indicates that the dominant wavelength of RGB LED systems are highly dependent on the optical power of individual LED sources. The dominant wavelength is physically related to the perceptual attribute Hue. The dominant wavelength can be defined as the intersection between a straight line drawn from the white reference (x=0.333; y=0.333) through the given color to boundaries of the CIE 1931 color space chromaticity diagram. An example of such straight line is shown in Fig. 1. The dominant wavelength of RGB LED systems decreases with decreasing the optical power of blue or

This article has been accepted for publication in a future issue of this journal, but has not been fully edited. Content may change prior to final publication. Citation information: DOI 10.1109/TPEL.2016.2581828, IEEE Transactions on Power Electronics



green LED at different rates. The thermal interactions of the RGB LED devices are highly complex, making precise color control very difficult particularly when dimming (i.e. changes of power and junction temperature) is involved.

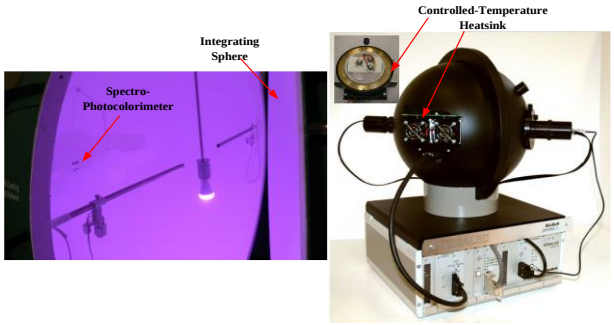


Fig 2 Diagram of experimental equipment

As shown in Figs. 5 and 6, at the controlled heatsink temperature of 25 $^0$C, the chromaticity coordinates ($x$,$y$) are about (0.3474,0.2345) and the dominant wavelength of the RGB LED lamp is 546.9 nm. When the heatsink temperature is 65 $^0$C, the chromaticity coordinates ($x$,$y$) decrease to (0.3058,0.2244), and dominant wavelength increases to 563.8 nm. These practical results highlight the important fact that color properties of RGB LED systems are highly dependent on thermal effects.

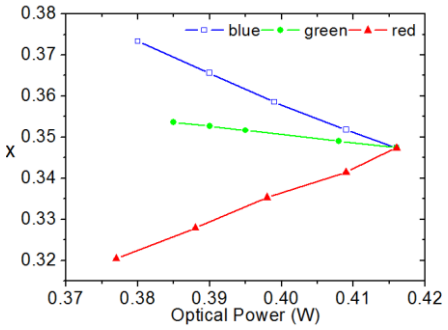


(a)

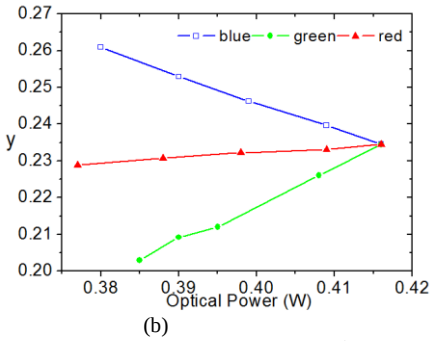


(b)

Fig 3 Measured the chromaticity coordinates ($x$,$y$) of RGB LED systems as function of a change in the optical power of the red, green, or blue LEDs inside RGB LED systems

Fig 7 (a) show the color deviation of $\Delta uv$ as the light intensity of individual LED source changes. At a color point of the optical power of 0.416 W, a variation of 3% on the light intensity of individual green LED source can lead to the mixed color shift by $\Delta uv$=0.006 of RGB LED systems, which is already outside the specification of LED sources [16]. This is a very small light intensity change compared with the variability in nominally indentical LED sources. For example, the minimum and typical optical power of Lumileds LED (LXML-PM01-0070) are 70 mW and 79 mW respectively [17]. The optical variability in nominally indentical LEDs is about 11.3%. Fig 7(b) shows the measured change in color point of $\Delta uv$ as the heatsink temperaure changes in increments of 10 $^0$C. A shift in the heatsink temperature of only 9 $^0$C can move the color point by $\Delta uv$=0.006. The reason on the color deviation is the reduction of the light output of RGB LED systems due to the thermal effect. Different LED sources could reduce their light intensity with increasing temperature at different rates according to their characteritic temperature values [2]. A high characteristic temperature implies that the light intensity is weakly dependent on junction temperature, which is a desirable feature. If it is possible to select LED source with high characteristic temperature, the color stability of the light output from RGB LED systems with temperature could be significantly improved.

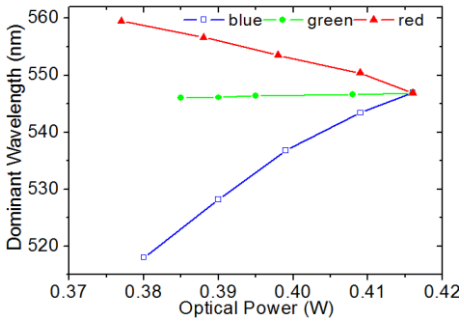


Fig 4 Measured the dominant wavelength of RGB LED systems as function of a change in the optical power of the red, green, or blue LEDs inside RGB LED systems

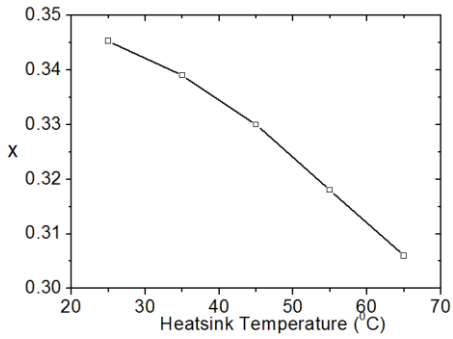


(a)

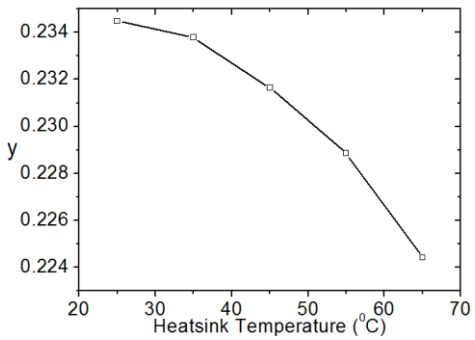


(b)

Fig 5 Measured the chromaticity coordinates ($x$,$y$) of RGB LED systems as function of heatsink temperature

This article has been accepted for publication in a future issue of this journal, but has not been fully edited. Content may change prior to final publication. Citation information: DOI 10.1109/TPEL.2016.2581828, IEEE Transactions on Power Electronics



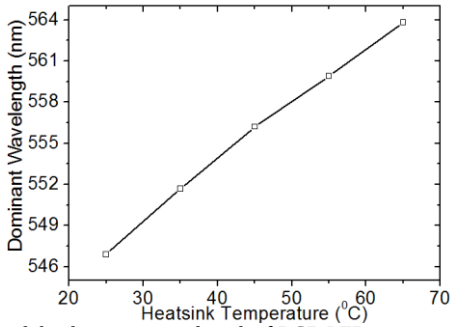


Fig 6 Measured the dominant wavelength of RGB LED systems as function of heatsink temperature

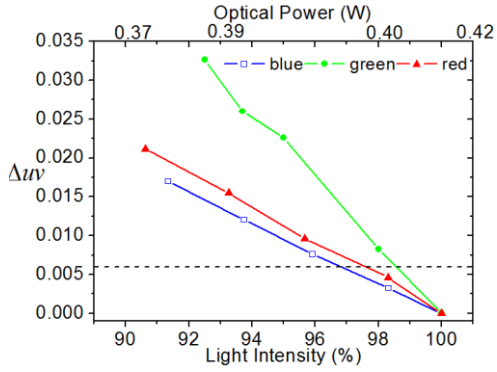


(a)

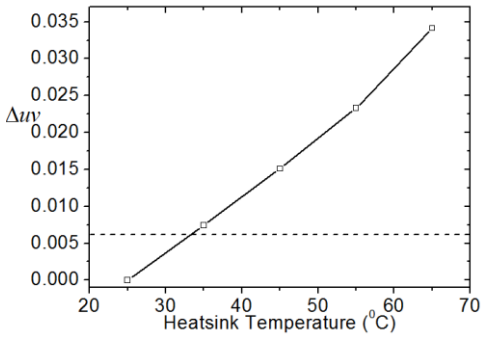


(b)

Fig 7 (a)Measured color deviation of RGB LED systems as a function of optical power of the red, green, or blue LEDs in the RGB LED lamp and (b) as a function of heatsink temperature

The mixed color point of an LED system is dependent on both its junction temperature as well as the amplitude of its light output of the invididual LED source. With the three LED sources inside the lamp sharing the same heatsink and driver together, but individually controlled, there will be thermal influence of one LED source on the color property of the other. In other words, there is thermal interdependence on the colors of the three LED sources. This thermal coupling effect should be carefully treated and should not be ignored in the design of RGB LED systems. Otherwise, there will always be an undesired change of the color in the process of adjusting brightness regardless of which control approach is adopted. It must be mentioned that a ±0.006 of $\Delta uv$ deviation within the desired color coordinates value is often cited as an acceptable error in solid state lighting and is considered non-perceivable. Nevertheless, it is found that existing approaches do not take into consideration the abovementioned factors and still possess perceivable color deviation.

### *B Existing Linear Color Control Approaches for RGB LED Systems*

Currently, approaches adopted in performing the color mixing in such lamps with red, green and blue LED sources are generally based on simple linear color averaging of the three LED sources. Any color can be matched by a linear combination of three color. This is fundamental to colorimetry and is Grassman's law of color mixture [19][20]. So a total tristimulus values ($X_T$,$Y_T$,$Z_T$) can be matched by ($X_R$,$Y_R$,$Z_R$) units of red, ($X_G$,$Y_G$,$Z_G$) units of green, ($X_B$,$Y_B$,$Z_B$) units of blue. The units can be measured in any form that quantifies light power in the following

$$\begin{cases} X_T\left(D_R,D_G,D_B\right)=X_R(D_R)+X_G(D_G)+X_B(D_B) \\ Y_T\left(D_R,D_G,D_B\right)=Y_R(D_R)+Y_G(D_G)+Y_B(D_B) \\ Z_T\left(D_R,D_G,D_B\right)=Z_R(D_R)+Z_G(D_G)+Z_B(D_B) \end{cases} \quad (4)$$

where $D_R$, $D_G$ and $D_B$ are duty cycles, and $X_R$, $X_G$ and $X_B$ are tristimulus values of the red, green and blue LED sources, respectively. $X_T$, $Y_T$ and $Z_T$ are the total tristimulus values of the mixed color. The chromaticity stablity of RGB LED systems is largely dependent on the junction tempeature $T_{J,R}$, $T_{J,G}$ and $T_{J,B}$ of the red, green and blue LED sources respectively. The junction temperature $T_{J,R}$ and tristimulus value $X_R$ of the red LED are incorrectly assumed to be only dependent on the operatinig conditions $D_R$ and not related to the operated status $D_G$ and $D_B$ of other two LEDs sources based on existing linear color model for RGB LED systems [19],[20].

The main problem with existing linear approaches is that they are rather simplistic by ignoring non-ideal characteristics such as the effect of temperature change on tristimulus values, and the thermal interdependency among the three LED sources. Without proper consideration of the actual dynamics of luminous flux, current, temperature, and duty cycle change, the achievable tristimulus values control will be inaccurate. Such errors are significant especially if wide-range dimming and precise color control are required since the temperature variation in such operations is large. Inaccuracy of the linear approach can be seen from the results plotted in Fig. 8, which shows the measured and calculated tristimulus values of the RGB LED system for a range of optical power. The calculated results are obtained with the use of (4). It is evident from the data that there are significant deviations between the calculated and measured tristimulus values. The errors increase with increasing optical power.

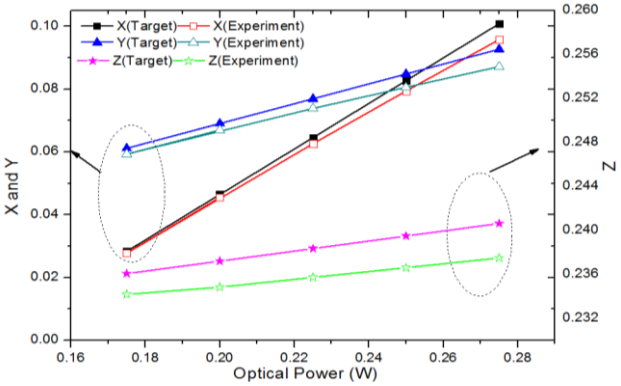


Fig 8 Measured and calculated tristimulus values ($X$,$Y$,$Z$) of RGB LED systems for different optical power based on the linear approach

This article has been accepted for publication in a future issue of this journal, but has not been fully edited. Content may change prior to final publication. Citation information: DOI 10.1109/TPEL.2016.2581828, IEEE Transactions on Power Electronics



## III. NEW NONLINEAR COLOR MODEL FOR RGB LED SYSTEMS

The junction temperature of a RGB LED system could affect the color as reflected by the variations of tristimulus values ($X,Y,Z$) [3]. Fig. 9 shows a basic thermally-coupled model of a RGB LED system with the RGB LEDs mounted on the same heatsink. $R_{GR}$, $R_{BR}$ and $R_{BG}$ are thermal resistance between green and red LEDs, blue and red LEDs, blue and green LEDs , respectively. $R_R$, $R_B$ and $R_G$ are thermal resistance between the corresponding LEDs and the heatsink. Generally, the junction temperature of an LED is affected by the current level, driving technique, heatsink size, and ambient temperature. In the case of a RGB LED system, the junction temperature of the individual LED source will be affected by the operating states of the other LED sources since the LEDs share the same heatsink. The thermal interdependency will be accounted for in the nonlinear color model.

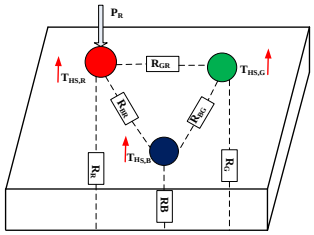


Fig 9 Thermally-coupled model of a RGB LED system.

### *A Practical Operating Range of Dimming and Color Control for Tri-color systems:*

The empirical nonlinear color model of a RGB LED system is built upon measured results obtained from the LED sources through the following steps. PWM drive is adopted in the procedure.

1) Mount the red, green and blue LEDs on the same heatsink and set their current amplitudes identically at 0.35 A.
2) Cover the green and blue LED sources with a black rubber sheet which prevents their light from being emitted into space whilst they can generate thermal energy into the heatsink. The minimum and maximum thermal energy that the green and blue LED sources can contribute to a RGB LED system occur when they are fully turned off at ($D_G = 0$, $D_B = 0$) and fully turned on at ($D_G = 1$, $D_B = 1$), respectively. The measurement of the tristimulus values ($X_R, Y_R, Z_R$) of the red LED source with respect to the operating condition of the green and blue LED sources will be performed under these two boundary conditions. Fig.10 shows the tristimulus values ($X_R, Y_R, Z_R$) versus the duty ratio $D_R$ of the red LED in both conditions of ($D_G = 0$, $D_B = 0$) and ($D_G = 1$, $D_B = 1$). Clearly, the maximum and minimum tristimulus values ($X_R, Y_R, Z_R$) from the red LED source occur at ($D_G = 0$, $D_B = 0$) and ($D_G = 1$, $D_B = 1$) as heat energy contributed by the green and blue LED sources is at its lowest and highest, respectively. The operating range of the red LED source at different operating conditions of the green and blue LED sources (i.e., $0 < D_G + D_B < 2$) should occur between maximum and minimum curves.
3) By covering the red and green LED sources with the black rubber sheet, the same measurement process is repeated on the blue LED sources. Fig. 11 shows the tristimulus values ($X_B, Y_B, Z_B$) versus the duty ratio $D_B$ of the blue LED source in both conditions of ($D_R = 0$, $D_G = 0$ when the red and green LED sources are fully off) and ($D_R = 1$, $D_G = 1$ when the red and green LED sources are fully on).
4) The same measurement process is repeated on the green LED sources. Fig. 12 shows the tristimulus values ($X_G, Y_G, Z_G$) versus duty ratio $D_G$ of the green LED source in both conditions of ($D_R = 0$, $D_B = 0$ when the red and blue LED sources are fully off) and ($D_R = 1$, $D_B = 1$ when the red and blue LED sources are fully on).

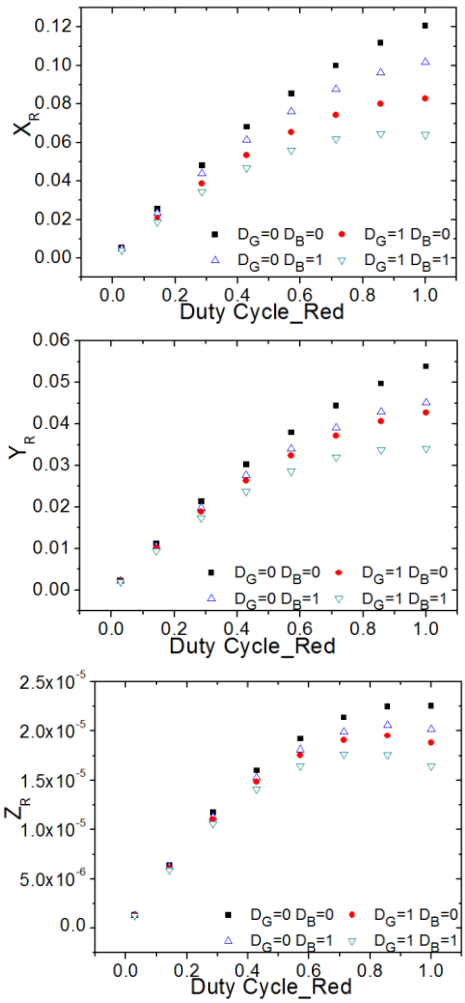


Fig. 10. Experimental values of tristimulus values ($X_R, Y_R, Z_R$) of the red LED source when the green and blue LED sources are fully off and fully on at different boundary conditions ($D_G = 0$ and $D_B = 0$; $D_G = 0$ and $D_B = 1$; $D_G = 1$ and $D_B = 0$; $D_G = 1$ and $D_B = 1$)

Fig. 13 depicts typical profiles of the nonlinear total tristimulus values ($X_T, Y_T, Z_T$) of a RGB LED system for different values of $D_T = (D_R + D_G + D_B)$ with their highest and lowest boundaries. For example, $D_T = 1$ means that ($D_R$, $D_G$, $D_B$) can be of any arbitrary combination provided that their sum is 1. For this $D_T = 1$ in Fig.13, the maximum of total tristimulus values ($X_T, Y_T, Z_T$) are (0.062, 0.041, 0.112). The RGB color space can be normalized so that the maximum is 1. The point with coordinates (1,1,1) corresponds to the system's brightest white. To uniquely specify the color space, a white reference point has to be specifed according to range of tristimulus values ($X_T, Y_T, Z_T$). Since this white point has to be normalized as (1,1,1) and this limit sets the full dimming range and color control for

This article has been accepted for publication in a future issue of this journal, but has not been fully edited. Content may change prior to final publication. Citation information: DOI 10.1109/TPEL.2016.2581828, IEEE Transactions on Power Electronics



the RGB system. There exist maximum values (i.e. $X_{T\text{-}max}$, $Y_{T\text{-}max}$ and $Z_{T\text{-}max}$ as shown in Fig. 13. The lowest value among these three maximum values will be chosed as 1.0. In the case of Fig. 13, $Y_{T\text{-}max}$ is 0.088, which is smaller than $X_{T\text{-}max}$ (0.105) and $Z_{T\text{-}max}$ (0.243). So $Y_{T\text{-}max}$ is set as 1.0 p.u. The full dimming range and color control of this RGB LED system is achievable only for the range of $Y_T$. These boundaries represent the operational dimming and color limits of a dimmable RGB LED system.

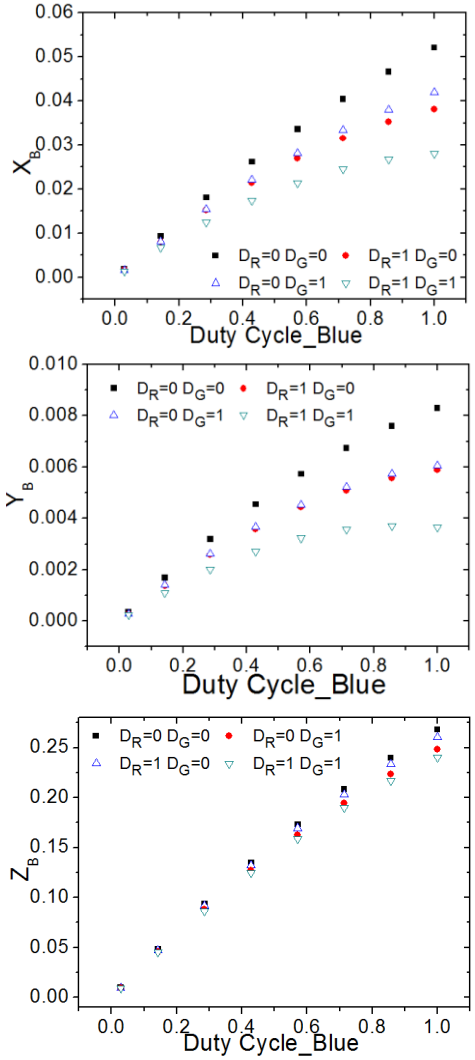


Fig. 11. Experimental values of tristimulus values ($X_B$,$Y_B$,$Z_B$) of the blue LED source when the red and green LED sources are fully off and fully on at different boundary conditions ($D_R$= 0 and $D_G$ = 0; $D_R$= 0 and $D_G$ = 1; $D_R$= 1 and $D_G$ = 0; $D_R$= 1 and $D_G$= 1)

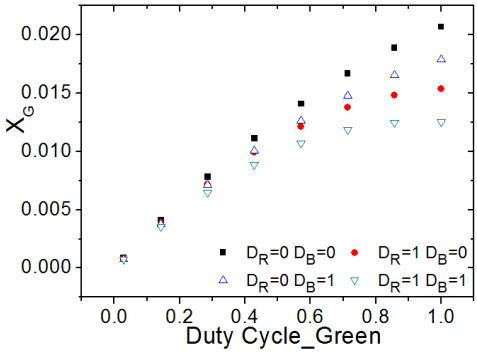


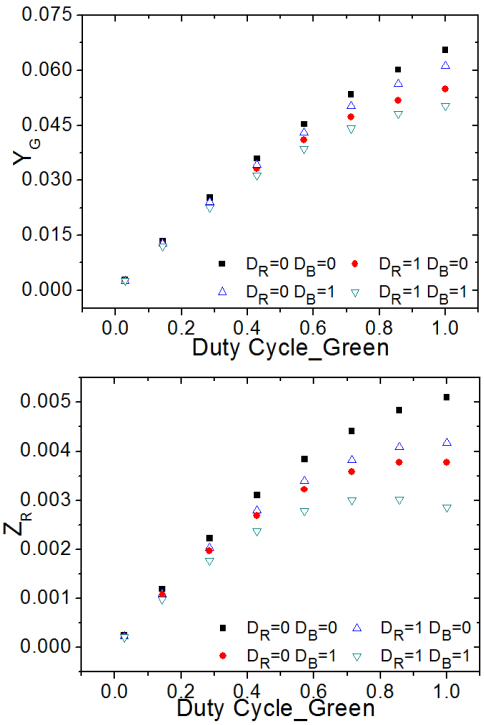


Fig.12. Experimental values of tristimulus values ($X_G$,$Y_G$,$Z_G$) of the green LED source when the red and blue LED sources are fully off and fully on at different boundary conditions ($D_R$ = 0 and $D_B$ = 0; $D_R$= 0 and $D_B$= 1; $D_R$= 1 and $D_B$ = 0; $D_R$= 1 and $D_B$ = 1)

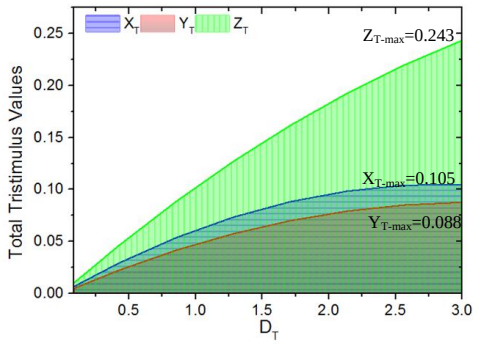


Fig. 13. Typical nonlinear total tristimulus values ($X_T$,$Y_T$,$Z_T$) behavior of a RGB LED system for different values of $D_T$

### *B Empirical Tristimulus Model of Individual LED inside RGB LED Systems*

Careful observation of the results shows that the tristimulus value ($X_R$,$Y_R$,$Z_R$) of the red LED source with consideration to the thermal contribution from the green and blue LED sources (Fig. 10) can be modeled using an polynomial function of the following form.

$$\begin{bmatrix} X_R(D_R,D_G,D_B) \\ Y_R(D_R,D_G,D_B) \\ Z_R(D_R,D_G,D_B) \end{bmatrix} = \begin{bmatrix} \alpha_{RX}(D_G,D_B) \\ \alpha_{RY}(D_G,D_B) \\ \alpha_{RZ}(D_G,D_B) \end{bmatrix} D_R^2 + \begin{bmatrix} \beta_{RX}(D_G,D_B) \\ \beta_{RY}(D_G,D_B) \\ \beta_{RZ}(D_G,D_B) \end{bmatrix} D_R \quad (5)$$

where $\alpha_{RX}$, $\beta_{RX}$, $\alpha_{RY}$, $\beta_{RY}$, $\alpha_{RZ}$, $\beta_{RZ}$ are variables related to the duty cycles of the green and blue LED sources. The results (Fig 10) can be fitted into polynomial function as shown in (5).

This article has been accepted for publication in a future issue of this journal, but has not been fully edited. Content may change prior to final publication. Citation information: DOI 10.1109/TPEL.2016.2581828, IEEE Transactions on Power Electronics



The gradient of each of these measured curves in Fig. 10 (a) determines the values of $\alpha_{RX}$ and $\beta_{RX}$ which vary with $D_R$. For the tristimulus value $X_R$ of red LED source, an operating area within the limits of $D_{G,min} \le D_G \le D_{G,max}$ and $D_{B,min} \le D_B \le D_{B,max}$ (for its companion green and blue LED sources) will generate a range of gradient values of $\alpha_{GRX,min}(\beta_{GRX,min}) \le \alpha_{RX}(\beta_{RX}) \le \alpha_{GRX,max}(\beta_{GRX,max})$ and $\alpha_{BRX,min}(\beta_{BRX,min}) \le \alpha_{RX}(\beta_{RX}) \le \alpha_{BRX,max}(\beta_{BRX,max})$. (Noted that $D_{G,min}=D_{B,min}=0$, $D_{G,max}=D_{B,max}=1$.) Likewise, for the tristimulus values $Y_R$ and $Z_R$ of red LED source, an operating range of $D_{G,min} \le D_G \le D_{G,max}$ and $D_{B,min} \le D_B \le D_{B,max}$ will generate a range of gradient values of $\alpha_{GRY,min}(\beta_{GRY,min}) \le \alpha_{RY}(\beta_{RY}) \le \alpha_{GRY,max}(\beta_{GRY,max})$, $\alpha_{BRY,min}(\beta_{BRY,min}) \le \alpha_{RY}(\beta_{RY}) \le \alpha_{BRY,max}(\beta_{BRY,max})$, $\alpha_{GRZ,min}(\beta_{GRZ,min}) \le \alpha_{RZ}(\beta_{RZ}) \le \alpha_{GRZ,max}(\beta_{GRZ,max})$ and $\alpha_{BRZ,min}(\beta_{BRZ,min}) \le \alpha_{RZ}(\beta_{RZ}) \le \alpha_{BRZ,max}(\beta_{BRZ,max})$, respectively. Therefore, $\alpha_{RX}(\beta_{RX})$, $\alpha_{RY}(\beta_{RY})$ and $\alpha_{RZ}(\beta_{RZ})$ of the red LED sources with the linear associations of $D_G$ and $D_B$ can be respectively expressed through interpolation inside the operating area within the practical limits as:

$$\begin{bmatrix} \alpha_{RX}(D_G,D_B) \\ \alpha_{RY}(D_G,D_B) \\ \alpha_{RZ}(D_G,D_B) \end{bmatrix} = \begin{bmatrix} \alpha_{RX,0} \\ \alpha_{RY,0} \\ \alpha_{RZ,0} \end{bmatrix} + \begin{bmatrix} \alpha_{RGX,\max}-\alpha_{RGX,\min} \\ \alpha_{RGY,\max}-\alpha_{RGY,\min} \\ \alpha_{RGZ,\max}-\alpha_{RGZ,\min} \end{bmatrix} \frac{(D_G-D_{G,\min})}{(D_{G,\max}-D_{G,\min})} + \begin{bmatrix} \alpha_{RBX,\max}-\alpha_{RBX,\min} \\ \alpha_{RBY,\max}-\alpha_{RBY,\min} \\ \alpha_{RBZ,\max}-\alpha_{RBZ,\min} \end{bmatrix} \frac{(D_B-D_{B,\min})}{(D_{B,\max}-D_{B,\min})} \quad (6)$$

$$\begin{bmatrix} \beta_{RX}(D_G,D_B) \\ \beta_{RY}(D_G,D_B) \\ \beta_{RZ}(D_G,D_B) \end{bmatrix} = \begin{bmatrix} \beta_{RX,0} \\ \beta_{RY,0} \\ \beta_{RZ,0} \end{bmatrix} + \begin{bmatrix} \beta_{RGX,\max}-\beta_{RGX,\min} \\ \beta_{RGY,\max}-\beta_{RGY,\min} \\ \beta_{RGZ,\max}-\beta_{RGZ,\min} \end{bmatrix} \frac{(D_G-D_{G,\min})}{(D_{G,\max}-D_{G,\min})} + \begin{bmatrix} \beta_{RBX,\max}-\beta_{RBX,\min} \\ \beta_{RBY,\max}-\beta_{RBY,\min} \\ \beta_{RBZ,\max}-\beta_{RBZ,\min} \end{bmatrix} \frac{(D_B-D_{B,\min})}{(D_{B,\max}-D_{B,\min})} \quad (7)$$

Equation (5) gives tristimulus value ($X_R$,$Y_R$,$Z_R$) of red LED source at any $D_R$, $D_G$ and $D_B$ values (of which $D_G$ and $D_B$ contribute to the thermal energy affecting the junction temperature of the red LED source). From the experimental results given in Fig. 10, the required parameters in (5) are extracted in the Table 1. Fitting these values into equation (5), the tristimulus value ($X_R$,$Y_R$,$Z_R$) for the red LED can be predicted for any $D_R$, $D_G$ and $D_B$. Fig. 14 gives a comparison of the experimentally measured tristimulus value ($X_R$,$Y_R$,$Z_R$) with including thermal energy affecting from blue and green LEDs and that calculated using equation (5). The maximum discrepancy between the two is around 9.2% and the minimum discrepancy is around 0.24%. The averaged discrepancy between the measured and calculated results is around 4.3%. Therefore, the proposed mathematical model provides reasonably accurate prediction.

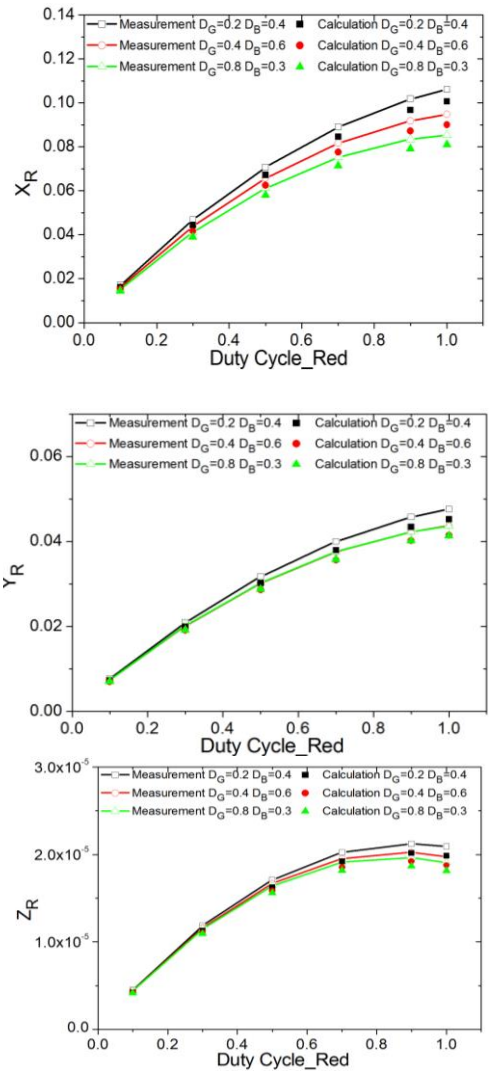


Fig. 14. Calculated and measured total tristimulus values ($X_R$,$Y_R$,$Z_R$) of red LED with different operating conditions

Likewise, the tristimulus values ($X_G$,$Y_G$,$Z_G$) and ($X_B$,$Y_B$,$Z_B$)of the green and blue LED sources also can be derived using the same method. Therefore, the tristimulus value ($X_G$,$Y_G$,$Z_G$) and ($X_B$,$Y_B$,$Z_B$)of the green and blue LED sources can be expressed as:

$$\begin{bmatrix} X_G(D_R,D_G,D_B) \\ Y_G(D_R,D_G,D_B) \\ Z_G(D_R,D_G,D_B) \end{bmatrix} = \left( \begin{bmatrix} \alpha_{GX,0} \\ \alpha_{GY,0} \\ \alpha_{GZ,0} \end{bmatrix} + \begin{bmatrix} \alpha_{GRX,\max}-\alpha_{GRX,\min} \\ \alpha_{GRY,\max}-\alpha_{GRY,\min} \\ \alpha_{GRZ,\max}-\alpha_{GRZ,\min} \end{bmatrix} \frac{(D_R-D_{R,\min})}{(D_{R,\max}-D_{R,\min})} + \begin{bmatrix} \alpha_{GBX,\max}-\alpha_{GBX,\min} \\ \alpha_{GBY,\max}-\alpha_{GBY,\min} \\ \alpha_{GBZ,\max}-\alpha_{GBZ,\min} \end{bmatrix} \frac{(D_B-D_{B,\min})}{(D_{B,\max}-D_{B,\min})} \right) D_G^2$$
$$+ \left( \begin{bmatrix} \beta_{GX,0} \\ \beta_{GY,0} \\ \beta_{GZ,0} \end{bmatrix} + \begin{bmatrix} \beta_{GRX,\max}-\beta_{GRX,\min} \\ \beta_{GRY,\max}-\beta_{GRY,\min} \\ \beta_{GRZ,\max}-\beta_{GRZ,\min} \end{bmatrix} \frac{(D_R-D_{R,\min})}{(D_{R,\max}-D_{R,\min})} + \begin{bmatrix} \beta_{GBX,\max}-\beta_{GBX,\min} \\ \beta_{GBY,\max}-\beta_{GBY,\min} \\ \beta_{GBZ,\max}-\beta_{GBZ,\min} \end{bmatrix} \frac{(D_B-D_{B,\min})}{(D_{B,\max}-D_{B,\min})} \right) D_G \quad (8)$$

This article has been accepted for publication in a future issue of this journal, but has not been fully edited. Content may change prior to final publication. Citation information: DOI 10.1109/TPEL.2016.2581828, IEEE Transactions on Power Electronics



$$\begin{bmatrix} X_B(D_R,D_G,D_B) \\ Y_B(D_R,D_G,D_B) \\ Z_B(D_R,D_G,D_B) \end{bmatrix} = \left[ \begin{bmatrix} \alpha_{BX,0} \\ \alpha_{BY,0} \\ \alpha_{BZ,0} \end{bmatrix} + \begin{bmatrix} \alpha_{BRX,\max} - \alpha_{BRX,\min} \\ \alpha_{BRY,\max} - \alpha_{BRY,\min} \\ \alpha_{BRZ,\max} - \alpha_{BRZ,\min} \end{bmatrix} \frac{\left(D_R - D_{R,\min}\right)}{\left(D_{R,\max} - D_{R,\min}\right)} + \begin{bmatrix} \alpha_{BGX,\max} - \alpha_{BGX,\min} \\ \alpha_{BGY,\max} - \alpha_{BGY,\min} \\ \alpha_{BGZ,\max} - \alpha_{BGZ,\min} \end{bmatrix} \frac{\left(D_G - D_{G,\min}\right)}{\left(D_{G,\max} - D_{G,\min}\right)} \right] D_B^2$$
$$+ \left[ \begin{bmatrix} \beta_{BX,0} \\ \beta_{BY,0} \\ \beta_{BZ,0} \end{bmatrix} + \begin{bmatrix} \beta_{BRX,\max} - \beta_{BRX,\min} \\ \beta_{BRY,\max} - \beta_{BRY,\min} \\ \beta_{BRZ,\max} - \beta_{BRZ,\min} \end{bmatrix} \frac{\left(D_R - D_{R,\min}\right)}{\left(D_{R,\max} - D_{R,\min}\right)} + \begin{bmatrix} \beta_{BGX,\max} - \beta_{BGX,\min} \\ \beta_{BGY,\max} - \beta_{BGY,\min} \\ \beta_{BGZ,\max} - \beta_{BGZ,\min} \end{bmatrix} \frac{\left(D_G - D_{G,\min}\right)}{\left(D_{G,\max} - D_{G,\min}\right)} \right] D_B \quad (9)$$

Table 1 Required parameters in (5) for the red LED source

| $\alpha_{RX,0}$ | $\beta_{RX,0}$ | $\alpha_{RGX,max}$ | $\alpha_{RGX,min}$ | $\alpha_{RBX,max}$ | $\alpha_{RBX,min}$ | $\beta_{RGX,max}$ | $\beta_{RGX,min}$ | $\beta_{RBX,max}$ | $\beta_{RBX,min}$ |
|---|---|---|---|---|---|---|---|---|---|
| -0.06743 | 0.18805 | -0.07332 | -0.06743 | -0.0733 | -0.06743 | 0.15624 | 0.18805 | 0.17508 | 0.18805 |
| $\alpha_{RY,0}$ | $\beta_{RY,0}$ | $\alpha_{RGY,max}$ | $\alpha_{RGY,min}$ | $\alpha_{RBY,max}$ | $\alpha_{RBY,min}$ | $\beta_{RGY,max}$ | $\beta_{RGY,min}$ | $\beta_{RBY,max}$ | $\beta_{RBY,min}$ |
| -0.02934 | 0.08314 | -0.03383 | -0.02934 | -0.03278 | -0.02934 | 0.079 | 0.08314 | 0.0755 | 0.08314 |
| $\alpha_{RZ,0}$ | $\beta_{RZ,0}$ | $\alpha_{RGZ,max}$ | $\alpha_{RGZ,min}$ | $\alpha_{RBZ,max}$ | $\alpha_{RBZ,min}$ | $\beta_{RGZ,max}$ | $\beta_{RGZ,min}$ | $\beta_{RBZ,max}$ | $\beta_{RBZ,min}$ |
| $-2.589*10^{-5}$ | $4.844*10^{-5}$ | $-2.774*10^{-5}$ | $-2.589*10^{-5}$ | $-2.705*10^{-5}$ | $-2.589*10^{-5}$ | $4.655*10^{-5}$ | $4.844*10^{-5}$ | $4.722*10^{-5}$ | $4.844*10^{-5}$ |

Table 2 Required parameters in (8) for the green LED source

| $\alpha_{GX,0}$ | $\beta_{GX,0}$ | $\alpha_{GRX,max}$ | $\alpha_{GRX,min}$ | $\alpha_{GBX,max}$ | $\alpha_{GBX,min}$ | $\beta_{GRX,max}$ | $\beta_{GRX,min}$ | $\beta_{GBX,max}$ | $\beta_{GBX,min}$ |
|---|---|---|---|---|---|---|---|---|---|
| -0.00928 | 0.02997 | -0.0099 | -0.00928 | -0.01371 | -0.00928 | 0.02776 | 0.02997 | 0.02906 | 0.02997 |
| $\alpha_{GY,0}$ | $\beta_{GY,0}$ | $\alpha_{GRY,max}$ | $\alpha_{GRY,min}$ | $\alpha_{GBY,max}$ | $\alpha_{GBY,min}$ | $\beta_{GRY,max}$ | $\beta_{GRY,min}$ | $\beta_{GBY,max}$ | $\beta_{GBY,min}$ |
| -0.03206 | 0.09763 | -0.03944 | -0.03206 | -0.03273 | -0.03206 | 0.09425 | 0.09763 | 0.09388 | 0.09763 |
| $\alpha_{GZ,0}$ | $\beta_{GZ,0}$ | $\alpha_{GRZ,max}$ | $\alpha_{GRZ,min}$ | $\alpha_{GBZ,max}$ | $\alpha_{GBZ,min}$ | $\beta_{GRZ,max}$ | $\beta_{GRZ,min}$ | $\beta_{GBZ,max}$ | $\beta_{GBZ,min}$ |
| $-3.78*10^{-3}$ | $8.88*10^{-3}$ | $-4.11*10^{-3}$ | $-3.78*10^{-3}$ | $-4.35*10^{-3}$ | $-3.78*10^{-3}$ | $8.29*10^{-3}$ | $8.88*10^{-3}$ | $8.12*10^{-3}$ | $8.88*10^{-3}$ |

Table 3 Required parameters in (9) for the blue LED source

| $\alpha_{BX,0}$ | $\beta_{BX,0}$ | $\alpha_{BRX,max}$ | $\alpha_{BRX,min}$ | $\alpha_{BGX,max}$ | $\alpha_{BGX,min}$ | $\beta_{BRX,max}$ | $\beta_{BRX,min}$ | $\beta_{BGX,max}$ | $\beta_{BGX,min}$ |
|---|---|---|---|---|---|---|---|---|---|
| -0.0158 | 0.0678 | -0.0211 | -0.0158 | -0.0170 | -0.0158 | 0.0592 | 0.0678 | 0.0589 | 0.0678 |
| $\alpha_{BY,0}$ | $\beta_{BY,0}$ | $\alpha_{BRY,max}$ | $\alpha_{BRY,min}$ | $\alpha_{BGY,max}$ | $\alpha_{BGY,min}$ | $\beta_{BRY,max}$ | $\beta_{BRY,min}$ | $\beta_{BGY,max}$ | $\beta_{BGY,min}$ |
| -0.00404 | 0.01233 | -0.00436 | -0.00404 | -0.00439 | -0.00404 | 0.012403 | 0.01233 | 0.01045 | 0.01233 |
| $\alpha_{BZ,0}$ | $\beta_{BZ,0}$ | $\alpha_{BRZ,max}$ | $\alpha_{BRZ,min}$ | $\alpha_{BGZ,max}$ | $\alpha_{BGZ,min}$ | $\beta_{BRZ,max}$ | $\beta_{BRZ,min}$ | $\beta_{BGZ,max}$ | $\beta_{BGZ,min}$ |
| -0.08188 | 0.34991 | -0.08456 | -0.08188 | -0.08472 | -0.08188 | 0.3328 | 0.3499 | 0.344931 | 0.34991 |

The total tristimulus values ($X_T$, $Y_T$, $Z_T$) of a RGB LED system is the combined tristimulus values of red, blue and green LED sources by considering (5) to (9).

*C Complete Tristimulus Values Model of RGB LED Systems*

From the experimental results given in Figs. 10-12, the required parameters of red, blue and green LED sources have been extracted and are tabulated in the following tables.

Putting the parameters of Table 1-3 into (5)-(9), the total tristimulus values ($X_T$, $Y_T$, $Z_T$) of the RGB LED system under consideration can be rewritten as (10), which provides the total tristimulus values ($X_T$, $Y_T$, $Z_T$) of the mixed color for a RGB LED system based on $D_R$, $D_G$ and $D_B$.

$$\begin{bmatrix} X_T(D_R,D_G,D_B) \\ Y_T(D_R,D_G,D_B) \\ Z_T(D_R,D_G,D_B) \end{bmatrix} = \begin{bmatrix} X_R(D_R,D_G,D_B) \\ Y_R(D_R,D_G,D_B) \\ Z_R(D_R,D_G,D_B) \end{bmatrix} + \begin{bmatrix} X_G(D_R,D_G,D_B) \\ Y_G(D_R,D_G,D_B) \\ Z_G(D_R,D_G,D_B) \end{bmatrix} + \begin{bmatrix} X_B(D_R,D_G,D_B) \\ Y_B(D_R,D_G,D_B) \\ Z_B(D_R,D_G,D_B) \end{bmatrix}$$
$$= \left[ \begin{bmatrix} -0.0674 \\ -0.0293 \\ -2.59*10^{-5} \end{bmatrix} + \begin{bmatrix} -0.00589 \\ -0.00449 \\ -1.55*10^{-6} \end{bmatrix} D_G + \begin{bmatrix} -0.00587 \\ -0.00344 \\ -1.16*10^{-6} \end{bmatrix} D_B \right] D_R^2 + \left[ \begin{bmatrix} 0.189 \\ 0.0831 \\ 4.84*10^{-5} \end{bmatrix} + \begin{bmatrix} -0.0318 \\ -0.00414 \\ -1.89*10^{-6} \end{bmatrix} D_G + \begin{bmatrix} -0.0129 \\ -0.00764 \\ -1.22*10^{-6} \end{bmatrix} D_B \right] D_R$$
$$+ \left[ \begin{bmatrix} -0.0093 \\ -0.0321 \\ -3.78*10^{-3} \end{bmatrix} + \begin{bmatrix} -0.00443 \\ -0.00738 \\ -3.3*10^{-4} \end{bmatrix} D_R + \begin{bmatrix} -0.000614 \\ -0.00067 \\ -5.7*10^{-4} \end{bmatrix} D_B \right] D_G^2 + \left[ \begin{bmatrix} 0.0299 \\ 0.0976 \\ 8.88*10^{-3} \end{bmatrix} + \begin{bmatrix} -0.000906 \\ -0.00338 \\ -5.9*10^{-4} \end{bmatrix} D_R + \begin{bmatrix} -0.00221 \\ -0.00375 \\ -7.6*10^{-4} \end{bmatrix} D_B \right] D_G$$
$$+ \left[ \begin{bmatrix} -0.0158 \\ -0.00404 \\ -0.0819 \end{bmatrix} + \begin{bmatrix} -0.0053 \\ -0.00032 \\ -0.00268 \end{bmatrix} D_R + \begin{bmatrix} -0.0012 \\ -0.00035 \\ -0.00284 \end{bmatrix} D_G \right] D_B^2 + \left[ \begin{bmatrix} 0.0678 \\ 0.0123 \\ 0.3499 \end{bmatrix} + \begin{bmatrix} -0.0086 \\ -0.00209 \\ -0.0171 \end{bmatrix} D_R + \begin{bmatrix} -0.0089 \\ -0.00188 \\ -0.00497 \end{bmatrix} D_G \right] D_B \quad (10)$$

*D Model Validation with Practical Measurements*

Fig. 15 gives a comparison of the measured and calculated total tristimulus values ($X_T$, $Y_T$, $Z_T$). The maximum discrepancy between the two is around 9.3% and it occurs at ($D_R$=0.2, $D_G$=0.4 and $D_B$=1). The minimum discrepancy is around 1.8% and it occurs at ($D_R$=0.2, $D_G$=0.4 and $D_B$=0). The averaged discrepancy between the measured and calculated results is around 4.3%. Therefore, the proposed nonlinear model provides reasonably accurate total tristimulus values ($X_T$, $Y_T$, $Z_T$) of a RGB LED system.

This article has been accepted for publication in a future issue of this journal, but has not been fully edited. Content may change prior to final publication. Citation information: DOI 10.1109/TPEL.2016.2581828, IEEE Transactions on Power Electronics



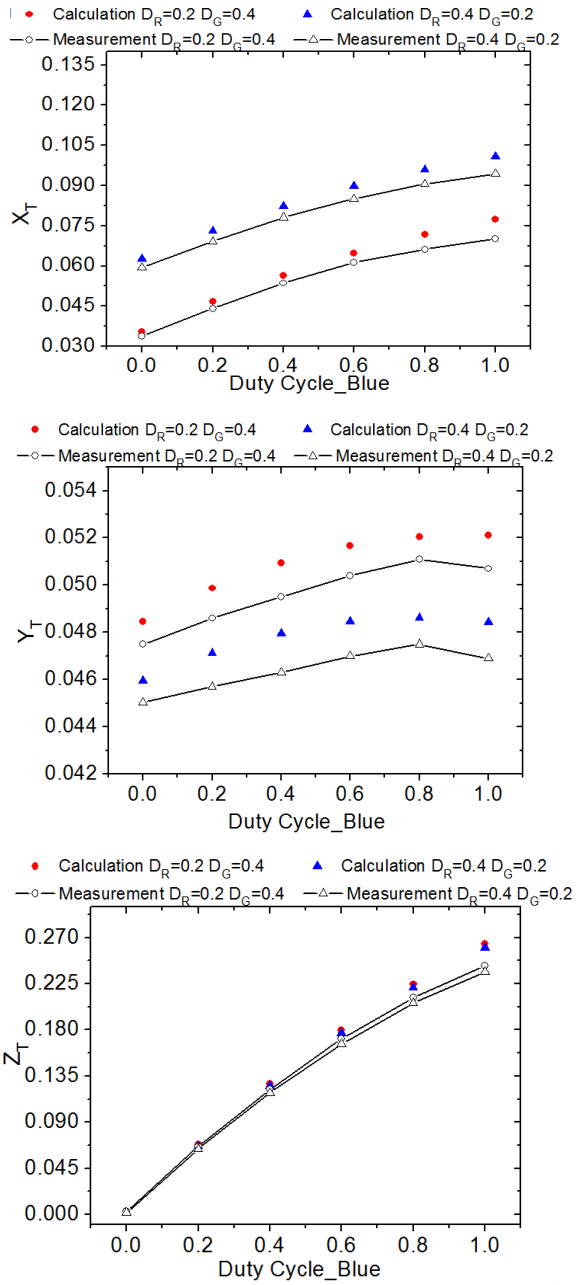


Fig. 15. Calculated and measured total tristimulus values ($X_T$,$Y_T$,$Z_T$) of mixed color for a RGB LED system with different operating conditions

## IV. PRACTICAL RESULTS AND DISCUSSIONS

In this section, the results of color predictions based on the linear and nonlinear color control are compared with practical measurements.

### *A Experimental Setup*

For a given desired set point of the CIE 1960 color space, the total tristimulus values ($X_T$,$Y_T$,$Z_T$) could be obtained using by the nonlinear color model. Three individual PWM signals are used to drive the MOSFET switches for dimming a red LED source (LXML_PD01_0030), green LED source (LXML_PM01_0040) and blue LED source (LXML_PR01_0175). The averaged current amplitudes of the red, blue and green LED sources are set precisely at 0.35 A. These three LED devices are mounted on the same heatsink which has a thermal resistance of 10.5 K/W. The mixed light of the RGB LED system is measured with a PMS-50 Spectro-Photocolorimeter as shown in Fig 2.

### *B Experimental Results and Discussion*

For comparison between the linear and the proposed nonlinear approaches, seven set points are chosen for practical evaluation. Fig. 16 shows the experimental values of the ($u$,$v$) of the RGB LED system that are obtained with the control based on the linear and nonlinear models for the seven different target set points. The measured color deviations of the linear control and linear control are included in the CIE 1960 color space. A shown in Fig 17, the maximum color deviation between the target set points and the experimental results obtained with the linear approach is 0.048 and the average color deviation is about 0.032. These deviations ($\Delta uv$ > 0.006) exceed the maximum color tolerance according to ANSI Standard C78.377 [16]. For control with the nonlinear model, the maximum color deviation is 0.01 and the averaged color deviation is about 0.006. Therefore, it is clearly shown that the nonlinear approach results in a more accurate color control of RGB LED systems. While control errors are still present with the nonlinear approach because of model and measurement inaccuracies, these errors in color is basically non-perceivable.

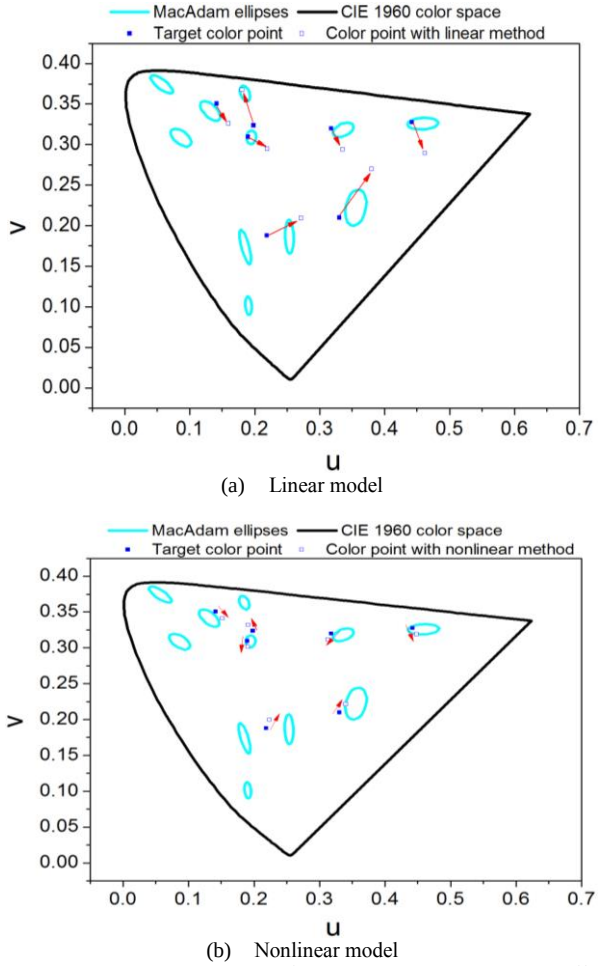


(a) Linear model

(b) Nonlinear model

Fig. 16. Measured color deviations of a RGB LED system based on different models (a) linear models (b) nonlinear models

This article has been accepted for publication in a future issue of this journal, but has not been fully edited. Content may change prior to final publication. Citation information: DOI 10.1109/TPEL.2016.2581828, IEEE Transactions on Power Electronics



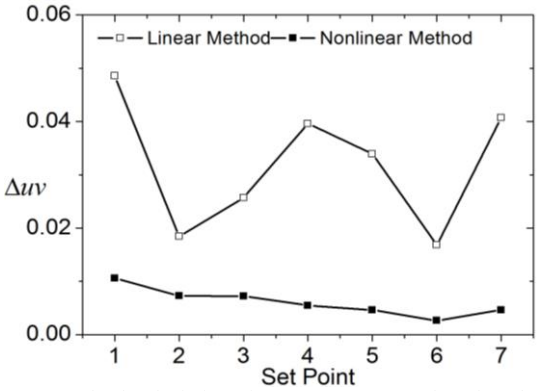


Fig 17 Measured color deviation of a RGB LED system based on the linear and nonlinear methods

## V CONCLUSIONS

Light science involves the complex interactions of heat, power, light and color. In this paper, a nonlinear tristimulus model and a control method for a RGB LED system are presented. This new RGB system model incorporates the highly nonlinear interactions of the mutual thermal effects and the differences of the characteristic temperature values of the RGB LEDs mounted on the same heatsink. The control method has been successfully and practically demonstrated for precise color control. The nonlinear method has been practically compared with the existing linear one. Experimental results have confirmed that the proposed approach is considerably more accurate than the existing linear approaches in obtaining the desired color points control in RGB LED systems.

## REFERENCES


[1] H. T. Chen, S. C. Tan, and S. Y. R. Hui, "Color variation reduction of GaN-based white light-emitting diodes via peak-wavelength stabilization", *IEEE Trans. Power Electron*., vol.29, no.7, pp. 3709-3719, Jul. 2014.

[2] S. Y. R. Hui and Y. X. Qin, "A general photo-electro-thermal theory for light-emitting-diode (LED) systems," *IEEE Trans. Power Electron.*, vol. 24, no. 8, pp.1967-1976, Aug. 2009.

[3] X. H. Qu, S. C. Wong, and C, K. Tse, "Temperature measurement technique for stabilizing the light output of RGB LED lamps", *IEEE Trans. Power Electron*., vol.59, no.3, pp. 661-670, Jul. 2010.

[4] S. K. Ng, K. H. Loo, Y. M .Lai, and C, K. Tse, "Color control system for RGB LED with application to light sources suffering from prolonged aging", *IEEE Trans. Industrial Electronics*., vol.61, no.4, pp. 1788-1798, Apr. 2014.

[5] S. M. Liu and Y. C. Chou, "Color calibration for a surrounding true-color LED display system by PWM controls," *IEEE Trans. Industrial Electronics*, vol.61, no.11, pp. 6244-6252, Nov. 2014.

[6] W. Feng, F. G. Shi, Y. He, and B. Zhao, "A switched supply tunable red-green-blue light emitting diode driver," *Rev. Sci. Instrum*, vol. 79, no. 4, pp. 044701,Apr. 2008.

[7] K. Modepalli and L. Parsa, "A scalable N-color LED driver using single inductor multiple current output topology," *IEEE Trans. Power Electron.*, vol. 31, no. 5, pp. 3773–3783, May 2016.

[8] A. T. L. Lee, J. K. O. Sin, and P. C. H. Chan, "Scalability of quasi-hysteretic FSM-based digitally controlled single-inductor dual-string buck LED driver to multiple strings", *IEEE Trans. Power Electron.*, vol. 29, no. 1, pp. 501–503, Jan. 2014.

[9] M. M. Sisto and J. Gauvin, "Accurate chromatic control and color rendering optimization in LED lighting systems using junction temperature feedback," *Proc. SPIE*, vol. 9190, pp. 919002-1-1919002-15, Sep. 2014.

[10] S. Beczkowski and S. M. Nielsen, "Current-voltage model of LED light sources," *IECON*, pp. 4533-4538, Oct. 2012.

[11] F. C. Wang, C. W. Tang, B. J. Huang. "Multivariable robust control for a red–green–blue LED lighting system," *IEEE Trans. Power. Electron*., vol. 25, no. 2, pp. 417-428, Feb. 2010.

[12] S. C. Tan, "General *n*-level driving approach for improving electrical-to-optical energy-conversion efficiency of fast-response saturable lighting devices," *IEEE Trans. Industral. Electron*., vol. 57, no. 4, pp. 1342–1353, Apr. 2010.

[13] H. T. Chen, S. C. Tan, and S. Y. R. Hui, "Nonlinear dimming and correlated color temperature control of bicolor white LED systems," *IEEE Trans. Power. Electron*., vol.30, no.12, pp. 6934-6947, Dec. 2015.

[14] A. T. L. Lee, H. T. Chen, S. C. Tan, and S. Y. R. Hui, "Precise Dimming and Color Control of LED Systems," *IEEE Trans. Power Electron.*, vol. 31, no. 1, pp. 65–80, Jan. 2016.

[15] S. Muthu, F. J. P. Schuurmans, and M. D. Pashley, "Red, green, and blue LEDs for white light illumination," *IEEE J. Sel. Top. Quantum. Electron.*, vol. 8, no. 2, pp.333-338, Mar. 2002.

[16] American National Standard, Specifications for Chromaticity of Solid State Lighting Products, ANSI C78.377 (American National Standards Institute, 2008).

[17] http://www.lumileds.com/uploads/265/DS68-pdf

[18] S. Y. R. Hui, H. T. Chen, and X. H. Tao, "An extended photoelectrothermal theory for LED systems - a tutorial from device characteristic to system design for general lighting [invited paper]," *IEEE Trans. Power. Electron*., vol.27, no.11, pp. 4571-4583, Nov. 2012.

[19] P. Deurenberg, C. Hoelen, J. V. Meurs, and J. Ansems, "Achieving color point stability in RGB multi-chip LED modules using various color control loops, " *Proc. SPIE, Fifth International Conference on Solid State Lighting*, vol. 5941, pp.63-74, Sep. 2005.

[20] T. P. Sun and C. H. Wang, "Specially designed driver circuits to stabilize LED light output without a photodetector, ", *IEEE Trans. Power Electron*., vol.27, no.9, pp. 4140-4152, Sep, 2012.


**Huanting Chen** (M'13) received the Ph.D degree in radio physics from Xiamen University, Xiamen, China, in 2010. He was a Joint Ph.D student at the Light & Lighting Laboratory, Catholic University College Gent, Belgium, from November 2009 to May 2010. He was a Senior Research Associate in the Department of Electronic Engineering, City University of Hong Kong, Hong Kong, in 2011. He is currently Postdoctoral Fellow in Department of Electrical and Electronic Engineering, The University of Hong Kong, Hong Kong. His research interests include solid-state lighting theory and technology.

**Siew-Chong Tan** (M'06–SM'11) received the B.Eng. (Hons.) and M.Eng. degrees in electrical and computer engineering from the National University of Singapore, Singapore, in 2000 and 2002, respectively, and the Ph.D. degree in electronic and information engineering from the Hong Kong Polytechnic University, Hong Kong, in 2005.

From October 2005 to May 2012, he worked as Research Associate, Postdoctoral Fellow, Lecturer, and Assistant Professor in Department of Electronic and Information Engineering, Hong Kong Polytechnic University, Hong Kong.

From January to October 2011, he was Senior Scientist in Agency for Science, Technology and Research (A*Star), Singapore. He is currently an Associate Professor in Department of Electrical and Electronic Engineering, The University of Hong Kong, Hong Kong. Dr. Tan was a Visiting Scholar at Grainger Center for Electric Machinery and Electromechanics, University of Illinois at Urbana-Champaign, Champaign, from September to October 2009, and an Invited Academic Visitor of Huazhong University of Science and Technology, Wuhan, China, in December 2011. His research interests are focused in the areas of power electronics and control, LED lightings, smart grids, and clean energy technologies.

Dr. Tan serves extensively as a reviewer for various IEEE/IET transactions and journals on power, electronics, circuits, and control engineering. He is an Associate Editor of the IEEE Transactions on Power Electronics. He is a coauthor of the book *Sliding Mode Control of Switching Power Converters: Techniques and Implementation* (Boca Raton: CRC, 2011).

**Albert T.L. Lee** received the BSc degree (Hons.) in Electrical Engineering from the University of Wisconsin, Madison in 1994, the MSc degree in Electrical and Computer Engineering from the University of Michigan, Ann Arbor in 1996, and the Ph.D. degree in Electronic and Computer Engineering at the Hong Kong University of Science and Technology (HKUST), Kowloon, Hong Kong in 2014.

Albert joined Intel Corporation, Hillsboro, Oregon in 1996 as a Senior Component Design Engineer and was involved in the development of Intel's P6 family microprocessors. In 2001, he served as a Senior Corporate Application Engineer in the System-Level Design Group at Synopsys Inc., Mountain View, California. In 2003, he joined the Hong Kong Applied Science and Technology Research Institute Company Ltd. and served as EDA Manager in the Wireline Communications Group. In 2006, he joined the Giant Electronics Limited as Hardware Design Manager and became Associate General Manager in 2008. Presently, he is a Research Associate in Department of Electrical and Electronic Engineering, The University of Hong Kong, Hong Kong. His research interests are focused in the areas of power electronics and control, LED lightings, and emerging LED driver technologies.

**Deyan Lin** (M'09) was born in China, in 1972. He received the B.Sc. and M.A.Sc. degrees from Huazhong University of Science and Technology, Wuhan, China, in 1995 and 2004, respectively, and the Ph.D. degree from the City University of Hong Kong, Kowloon, in 2012.

He is currently a Post-doctoral Fellow with the Department of Electrical and Electronic Engineering, The University of Hong Kong, Pokfulam, Hong Kong. From 1995 to 1999, he was a Teaching Assistant in the Electrical Engineering Department at Jianghan University, Wuhan, where he became a Lecturer later. From 2008 to 2009, he was a Senior Research Assistant with the City University of Hong Kong. His current research interests include wireless power transfer, LED lighting, memristors and modeling, control, simulation of gas-discharge lamps.

**S. Y. (Ron) Hui** (M'87-SM'94-F'03) received his BSc (Eng) Hons at the University of Birmingham in 1984 and a D.I.C. and PhD at Imperial College London in 1987. He has previously held academic positions at the University of Nottingham (1987–90), University of Technology Sydney (1991-92), University of Sydney (92-96), City University of Hong Kong (1996-2011). From July 2011, he holds the Chair Professorship at the University of Hong Kong. Since July 2010, he concurrently holds a part-time Chair Professorship at Imperial College London. He has published over 300 technical papers, including more than 210 refereed journal publications and book chapters. Over 60 of his patents have been adopted by industry. His inventions on wireless charging platform technology underpin key dimensions of Qi, the world's first wireless power standard, with freedom of positioning and localized charging features for wireless charging of consumer electronics. In Nov. 2010, he received the IEEE Rudolf Chope R&D Award from the IEEE Industrial Electronics Society, the IET Achievement Medal (The Crompton Medal) and was elected to the Fellowship of the Australian Academy of Technological Sciences & Engineering. He is the recipient of the 2015 IEEE William E. Newell Power Electronics Award.